Deriving the governing equation for a shock damper to model the unsteady flow caused by sudden valve closure and sudden demand change

Mohammad Bostan, Ali Akbar Akhtari and Hossein Bonakdari

ABSTRACT

The focus of this work is on deriving the governing equations for the 'shock damper', an instrument used in water flow systems. The shock damper is a mechanical tool with a single degree of freedom system that includes a tank, connecting pipe, mass, spring and damper. This tool serves as a boundary condition for characteristic line equations. Additional equations are included by considering the conservation of mass, momentum and energy. This system of equations is then explicitly solved at each time step. In order to illustrate how the shock damper performs, two gravity feed systems with and without a damper are considered. In the first system, the control valve suddenly shuts, and in the second system, rapid demand change occurs in one of the nodes to impose a water hammer condition. Subsequently, unsteady flow parameters such as minimum/maximum flow velocity and pressure are evaluated and a sensitivity analysis is carried out. The results demonstrate that despite being simple and economically efficient, the shock damper is highly capable of moderating unsteady flow characteristics.

Key words | shock damper, surge tank, unsteady flow effect, water hammer

Mohammad Bostan (corresponding author)
Ali Akbar Akhtari
Hossein Bonakdari
Department of Civil Engineering, College of Engineering,
Razi University,
Kermanshah,
Iran
E-mail: *bostancivil@gmail.com*

INTRODUCTION

One of the key factors to consider in designing a water distribution system is the effect of possible unsteady flow caused by a water hammer. A water hammer is a pressure surge or wave propagating at the speed of sound, which is created when a fluid (usually a liquid) in motion is forced to stop or change direction suddenly (momentum change). This phenomenon can occur for various reasons, including rapid valve opening and/or shutting, pump, joint or pipe failure, and using check valves. Water hammers cause intensive damage in some cases, making it a significant factor to keep in view while designing water distribution systems.

Two approaches to tackle this problem have been reported: (a) taking the necessary precautions to avoid a sudden change in flow velocity (or direction) that would cause a water hammer; and (b) equipping the water system with efficient tools to dampen the harmful impacts of a water hammer. As water hammers seem to be inevitable, the second approach is widely employed. Such tools (e.g., shock dampers) help depreciate the consequences of unsteady flow due to water hammers by compensating for any changes in flow pressure. Surge tanks and safety valves are the two kinds of water hammer damping equipment (Tijsseling 1996; Tijsseling *et al.* 1996). In order to simulate the dynamic behaviour of surge tanks, they are introduced as a boundary condition for characteristic line equations. Taking the conservation of mass, momentum and energy into account augments the number of equations in a system to n, where n is the number of unknown surge tank variables. Detailed discussions on this topic have been presented by Larock *et al.* (1999) and Skulovich *et al.* (2015, 2016). Safety valves are also applied as a boundary condition, and additional equations are derived to form a system

doi: 10.2166/aqua.2017.116

of equations. Niełacny (2004) modelled spring safety valves in a water distribution system with pumps.

High operational cost is a major concern with utilizing surge tanks. Despite being expensive, one-way surge tanks are unable to dampen the positive pressure wave caused by a water hammer. They are only capable of preventing the negative waves and column separation by injecting flow to the pipeline (Larock *et al.* 1999; Chamani *et al.* 2013; Fathi-Moghadam *et al.* 2013). Air surge tanks can handle both positive and negative waves, but they are costly (Larock *et al.* 1999; Kim 2008, 2010). On the other hand, safety valves have much lower installation and maintenance costs, yet they perform poorly in restraining positive waves and are incapable of hindering negative waves; thus, column separation and consequent damage to the system are inevitable (Bergant & Simpson 1995; Ghidaoui *et al.* 2005). For this reason, we aim to find a simple and economic alternative for handling both negative and positive waves.

This study focuses on the shock damper in an attempt to derive its governing equations and illustrate its effectiveness. According to the results, shock dampers are highly capable of moderating unsteady flow characteristics. The rest of this paper is structured as follows. The next section defines the problem under study, which includes deriving and solving the equations for the given boundary conditions. Then the performance of the proposed approach is demonstrated by solving a case study. The results are depicted in the following section and the conclusions comprise the final section.

PROBLEM DEFINITION

The current study focuses on the proposed instrument, i.e., the shock damper. It is capable of encountering positive and negative waves caused by water hammers. In this section, the shock damper is demonstrated, the governing equation is derived, boundary conditions are considered and the resulting system of equations is solved.

Shock damper

A shock damper consists of a damper, spring, mass, tank and joint (Figure 1). The spring, damper and mass perform together as a vibrant system with a single degree of freedom (vertically) when positive or negative waves occur. The spring here is pre-pressed to capture sufficient force, which is used to balance the force caused by the pressure head. In the case of positive waves, the excessive pressure imposed on the spring compresses it further, storing potential energy. This potential energy protects the rest of the water distribution system from water hammer effects (waves). When a negative wave hits the shock damper, the pre-pressed spring elongates and water stored in the shock damper's tank is injected into the flow to compensate for the negative pressure. This helps prevent column separation and subsequent damage to the system. Theoretically, after a water hammer occurs, an infinite number of periodic waves must be created in the system. However, this is never the case as a result of friction and energy depreciation. The shock damper acts to accelerate the process of water hammer wave depreciation. Figure 1 illustrates a shock damper and its components, including the (1) damper, (2) spring, (3) mass, (4) joint and (5) tank.

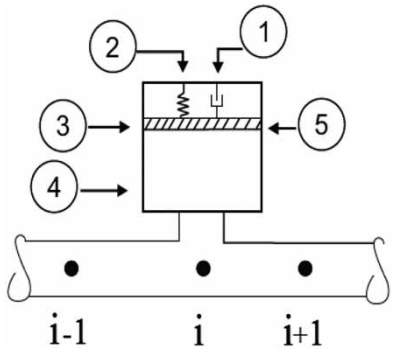

Figure 1 | Shock damper and its components.

Governing equations

To simulate the condition of unsteady flow in the system, a pair of partial differential equations (Equations (1) and (2)) are used. These equations are obtained by considering the conservation of mass and momentum for a moving control volume as an element of the pipeline (Chaudhry 1979; Wylie 1984)

$$\frac{\partial V}{\partial t} + g\frac{\partial H}{\partial x} + \frac{fV|V|}{2D} = 0 \quad (1)$$

$$\frac{\partial H}{\partial t} + \frac{a^2}{g}\frac{\partial V}{\partial x} = 0 \quad (2)$$

where H is the piezometric head and V is the flow velocity, both of which are functions of time (t) and space (x); a is the speed of sound wave propagation in the flow; g is the gravitational acceleration; D is the pipe diameter; and f is the Darcy–Weisbach coefficient. All dimensions are in standard SI units. One of the most widely-used approaches for solving equations similar to Equations (1) and (2) is the characteristic line method (Chaudhry 1979). In this method, the solution space is discretized to a finite number of nodes including intermediate and boundary nodes.

Intermediate nodes

The discretized forms of the equations for intermediate nodes in unsteady flow condition are represented below (Chaudhry 1979; Larock *et al.* 1999):

$$Q_i^{n+1} = \frac{1}{2}\begin{bmatrix} (Q_{i-1}^n + Q_{i+1}^n) + \dfrac{gA}{a}(H_{i-1}^n - H_{i+1}^n) \\ +\dfrac{g}{a}\Delta t(Q_{i-1}^n - Q_{i+1}^n)\sin\alpha \\ -\dfrac{f\Delta t}{2DA^2}(Q_{i-1}^n|Q_{i-1}^n| + Q_{i+1}^n|Q_{i+1}^n|) \end{bmatrix} \tag{3}$$

$$H_i^{n+1} = \frac{1}{2}\begin{bmatrix} (H_{i-1}^n + H_{i+1}^n) + \dfrac{a}{gA}(Q_{i-1}^n - Q_{i+1}^n) \\ +\dfrac{\Delta t}{A}(Q_{i-1}^n + Q_{i+1}^n)\sin\alpha \\ \dfrac{a}{g}\dfrac{f\Delta t}{2DA^2}(Q_{i-1}^n|Q_{i-1}^n| + Q_{i+1}^n|Q_{i+1}^n|) \end{bmatrix} \tag{4}$$

In the above equations, H_i^{n+1} and Q_i^{n+1} are the piezometric head and flow rate in node i at time step $n+1$, respectively, and A is the pipe's cross section.

Boundary conditions

To derive the governing equations of a shock damper, a gravity feed system is considered. Such a system includes a pipe, tank, valve and shock damper, each with a specific equation (boundary condition).

Reservoir

The following equations are considered for a reservoir with constant head (H_{up}^0) located at the beginning of a pipeline with i = 1 node (Larock *et al.* 1999):

$$H_i^{n+1} = H_{up}^0 \tag{5}$$

$$Q_i^{n+1} = Q_{i+1}^n + \frac{gA}{a}(H_{up}^0 - H_{i+1}^n) - \frac{f\Delta t}{2DA^2}Q_{i+1}^n|Q_{i+1}^n| \tag{6}$$

If the reservoir is located at the downstream end (node i = N) with constant head (H_{down}^0), the following equations are considered:

$$H_i^{n+1} = H_{down}^0 \tag{7}$$

$$Q_i^{n+1} = Q_{i+1}^n - \frac{gA}{a}(H_{down}^0 - H_{i-1}^n) - \frac{f\Delta t}{2DA^2}Q_i^n|Q_i^n| \tag{8}$$

Valve at node number i = B_v

Assuming the valve is located in the pipeline at node number $i = B_v$, the boundary condition equations for the valve that suddenly closes at time T_c are as follows (Larock *et al.* 1999):

$$Q_{i+1}^{n+1} = Q_i^{n+1} = \frac{2B'}{K_V}\left(-1 + \sqrt{\left(1 + \frac{4C_v^n K_v}{B'^2}\right)}\right) \tag{9}$$

$$C^+: \quad H_i^{n+1} = \frac{1}{C_2}\left(C_i^n - \frac{Q_i^{n+1}}{A}\right) \tag{10}$$

$$C^-: \quad H_{i+1}^{n+1} = \frac{1}{C_4}\left(\frac{Q_{i+1}^{n+1}}{A} - C_2^n\right) \tag{11}$$

$$\frac{1}{K_v} = 0.0088\, e^{[0.0088\theta(t)]} \tag{12}$$

$$\theta(t) = \theta_0\left(1 - \frac{t}{T_c}\right) \qquad 0 \le t \le T_c$$
$$\theta(t) = 0 \qquad t > T_c \tag{13}$$

$$B' = 2g\left(\frac{1}{C_1} + \frac{1}{C_2}\right) \tag{14}$$

$$C_1 = \frac{g}{a_1} \quad , \quad C_2 = \frac{g}{a_2} \tag{15}$$

$$C_v^n = 2g\left(\frac{C_1^n}{C_1} + \frac{C_2^n}{C_2}\right) \tag{16}$$

$$C_i^n = \frac{Q_{i-1}^n}{A} + \frac{g}{a}H_{i-1}^n - \frac{f\Delta t}{2DA^2}Q_{i-1}^n\left|Q_{i-1}^n\right| + \frac{g}{aA}\Delta t\ Sin\ \theta\ \ Q_{i-1}^n \tag{17}$$

$$C_2^n = \frac{Q_{i+2}^n}{A} + \frac{g}{a}H_{i+2}^n - \frac{f\Delta t}{2DA^2}Q_{i+2}^n\left|Q_{i+2}^n\right| - \frac{g}{aA}\Delta t\ Sin\ \theta\ \ Q_{i+2}^n \tag{18}$$

where Q_i^{n+1}, Q_{i+1}^{n+1} are the flow rates at the valve's node and the node after the valve at time step $n+1$, which can be calculated with Equation (9). Moreover, the pressure head values at the nodes in each time step (H_{i+1}^{n+1}, H_i^{n+1}) are calculated with Equations (10) and (11) using the C^+ and C^- characteristic lines concept. Equation (12) calculates the valve head loss coefficient (K_v) as a function of the valve's opening percentage ($\theta(t)$), assuming the valve closes as a linear function of time (Equation (13)). Equations (14) and (16) calculate the values of B', C_V^n that will be used in other equations. In Equation (15), the values of a_1, a_2 represent the wave speeds in the pipe before and after the valve. The values of C_1^n, C_2^n are calculated with Equations (17) and (18) and are then used in other equations. The other parameters were defined previously.

Shock damper at node number i = B_{sh}

As shown in Figure 2, it is assumed the shock damper is located at node number $i = B_{sh}$. Expanding the conservation of mass for this node yields:

$$Q_i^{n+1} = Q_{i+1}^{n+1} + Q_c^{n+1} \tag{19}$$

where Q_c^{n+1} is the flow rate from the main pipe to the shock damper joint at time step $n+1$. Whenever flow enters the shock damper it is assumed to be a positive flow rate, otherwise it is negative.

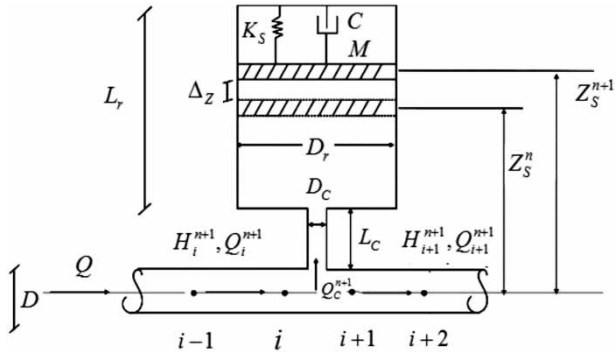

Figure 2 | Shock damper as a boundary condition.

Next, the conservation of energy is expanded for node i. If the space interval used is small enough, the energy depreciation due to friction in the distance between nodes i and $i+1$ along the pipeline is deemed negligible. By using the mean of the values in each time step and assuming the junction pipe is a control volume for solving force equilibrium equation, the control volume is influenced by the force $((Z_s^{n+1} + Z_s^n/2) + (P_0^{n+1} + P_0^n/2\gamma))\gamma A_C$ from the top and force $(H_i^{n+1} + H_i^n/2)\gamma A_C$ from the bottom. Friction force $(fL_c/\ 4gD_cA_c^2)(Q_c^n|Q_c^n| + Q_c^{n+1}|Q_c^{n+1}|)$ also acts along the junction pipe, so by considering the mentioned forces, the force equilibrium is developed as follows:

$$\begin{aligned}\frac{L_C}{gA_c\Delta t}(Q_c^{n+1} - Q_c^n) &= \frac{H_i^{n+1} + H_i^n}{2} \\ &- \frac{fL_c}{4gD_cA_c^2}\ (Q_c^n|Q_c^n| + Q_c^{n+1}|Q_c^{n+1}|) \\ &- \frac{Z_s^{n+1} + Z_s^n}{2} - \frac{P_0^{n+1} + P_0^n}{2\gamma}\end{aligned} \tag{20}$$

(here, only undefined parameters define other previously defined parameters), where L_c is the length of the joint; Z_s^n is the mass level proportional to the pipe axis in each time step; and P_0^n is the pressure imposed on the moving mass at each time step. By using the continuity principle, Z_s^n can be calculated as follows:

$$Z_s^{n+1} = Z_s^n + \frac{\Delta t}{2A_r}(Q_c^{n+1} + Q_c^n) \tag{21}$$

Figure 3 shows a free body diagram of any element of mass in the tank. Applying Newton's second law of

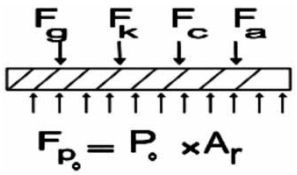

Figure 3 | Free diagram of motion mass.

motion along the vertical axis leads to:

$$P_0^{n+1}A_r = M\ddot{Z}^{n+1} + C\dot{Z}^{n+1} + K_s(Z_s^{n+1} - Z^0) + K_s\Delta_0 + Mg \tag{22}$$

where M is the moving mass; C is the damping coefficient; A_r is the cross section of the shock damper's tank; K_s is the spring stiffness factor; Z^0 is the initial mass height of the pipe's axis at $t = 0$; and Δ_0 is the distance over which the spring has been compressed at $t = 0$. The forces are defined as follows: gravity force $F_g = Mg$; spring force $F_K = K_s(Z_s^{n+1} - Z^0 + \Delta_0)$; damping force $F_c = C\dot{Z}^{n+1}$ and inertia force $F_a = M\ddot{Z}^{n+1}$. The above equations represent the vibration of a system with a single degree of freedom (vertically). $\dot{Z}^{n+1}$ *and* $\ddot{Z}^{n+1}$ in the above equation are the acceleration and velocity of the flow mass, respectively, and are calculated as:

$$\dot{Z}^{n+1} = \frac{Z_s^{n+1} - Z_s^n}{\Delta t} \tag{23}$$

$$\ddot{Z}^{n+1} = \frac{\dot{Z}^{n+1} - \dot{Z}^n}{\Delta t} \tag{24}$$

By using Equation (21) and the relations between position, velocity and acceleration, the velocity ($\dot{Z}^{n+1}$) and acceleration ($\ddot{Z}^{n+1}$) of the mass in the tank can be calculated based on the flow rate in the joint using the continuity principle as follows:

$$\dot{Z}^{n+1} = \frac{Q_c^n + Q_c^{n+1}}{2A_r} \tag{25}$$

$$\ddot{Z}^{n+1} = \frac{Q_c^n + Q_c^{n+1}}{\Delta t\, A_r} \tag{26}$$

The flow rate and head at nodes i and $i+1$ (Q_i^{n+1}, Q_{i+1}^{n+1}, H_i^{n+1} and H_{i+1}^{n+1}) can be estimated by considering the characteristic line equations C^- and C^+ and the equations below:

$$Q_i^{n+1} = \left(C_1^n - \frac{g}{a}H_i^{n+1}\right)A \tag{27}$$

$$Q_{i+1}^{n+1} = \left(C_2^n + \frac{g}{a}H_{i+1}^{n+1}\right)A \tag{28}$$

$$H_i^{n+1} = \frac{(C_1^n - C_2^n - (Q_c^{n+1}/A))}{2g/a} \tag{29}$$

$$H_{i+1}^{n+1} = H_i^{n+1} \tag{30}$$

In the above equations, C_1^n and C_2^n are derived with Equations (17) and (18) (with node number $i = B_{sh}$). In each time step the nine variables H_i^{n+1}, H_{i+1}^{n+1}, Q_i^{n+1}, Q_{i+1}^{n+1}, Q_c^{n+1}, $\dot{Z}^{n+1}$, $\ddot{Z}^{n+1}$, Z_s^{n+1} and P_0^{n+1} are computed with Equations (20)–(22) and (25)–(30).

Solving the system of equations for a shock damper

The system of equations defined in the previous section is used to simulate the behaviour of a shock damper when a water hammer occurs. The next step is to solve this difficult nonlinear and implicit system of equations. To do so, the term $(fL_c/4gD_cA_c^2)(Q_c^n|Q_c^n| + Q_c^{n+1}|Q_c^{n+1}|)$ in Equation (20) is replaced with $(fL_c/2gD_cA_c^2)(Q_c^n|Q_c^n|)$. By replacing H_i^{n+1}, H_{i+1}^{n+1}, Q_i^{n+1}, Q_{i+1}^{n+1}, $\dot{Z}^{n+1}$, $\ddot{Z}^{n+1}$, Z_s^{n+1} and P_0^{n+1} in Equation (20) with their corresponding values from Equations (21), (22) and (25)–(30), Equation (20) changes into an explicit linear form with Q_c^{n+1} as the only variable:

$$\alpha_1 Q_c^{n+1} = \alpha_2^n Q_c^n + \alpha_3^n \tag{31}$$

In the above equation, new parameters are introduced and defined as follows:

$$\alpha_1 = \left[\begin{array}{l} \dfrac{L_c}{gA_c\,\Delta t} + \dfrac{a}{2\,A\,g} + \dfrac{\Delta t}{4A_r} \\ + \dfrac{M}{2\gamma A_r^2 \Delta t} + \dfrac{C}{4\gamma A_r^2} + \dfrac{K_s \Delta t}{4\gamma A_r^2} \end{array}\right] \tag{32}$$

$$\alpha_2^n = \begin{bmatrix} \dfrac{L_c}{gA_c\,\Delta t} - \dfrac{\Delta t}{4A_r} + \dfrac{M}{2\gamma A_r^2} \\ -\dfrac{C}{4\gamma A_r^2} - \dfrac{K_s \Delta t}{4\gamma A_r^2} - \dfrac{fL_c}{2gA_c^2 D_c} Q_c^n \end{bmatrix} \tag{33}$$

$$\alpha_3^n = \begin{bmatrix} \dfrac{H_i^n}{2} + \dfrac{(C_1^n - C_2^n)a}{2g} - Z_s^n \\ -\dfrac{P_0^n}{2\gamma} - \dfrac{K_s \Delta_0 + Mg}{2\gamma A_r} \end{bmatrix} \tag{34}$$

CASE STUDIES

The efficiency of the proposed model is examined against two benchmark examples from the literature. The examples are solved in two scenarios: with and without a shock damper. The aim is to demonstrate the effect of installing a shock damper on the flow characteristics of such systems.

First case study (rapid valve closure)

The example involves transients caused by rapid valve closure downstream of a long conduit with an upstream reservoir (solved by Saikia & Sarma (2006) and Afshar & Rohani (2008)). A water hammer condition is created by shutting the downstream valve at $T_C = 4$ seconds. The initial system condition includes a constant flow rate in the pipe.

Scenario 1

In this case, the system is not equipped with a shock damper. The piezometric head in the tank is 600 ft; the main pipe diameter is 2 ft; the pipe length is 12,000 ft and the Darcy–Weisbach coefficient is $f = 0.02$ (for both steady and unsteady flow). The steady discharge is 12 ft^3/sec, the pressure wave velocity after valve closure is $a = 3{,}000$ ft/sec and Δx and Δt are assumed to be 3,000 ft and 1 sec, respectively.

Scenario 2

A shock damper is used in this scenario, which is located 50 ft upstream of the closure valve. The parameters related to the shock damper are:

$$M = 100\ \ lb, \quad C = 1.5 \times 10^8\ lb \cdot \sec/ft^{-1},$$
$$K_s = 1.4 \times 10^7\ lb/ft^{-1}, \quad Dr = 10\ ft,$$
$$Dc = 1\ ft, \quad Lr = 6\ ft \quad and \quad Lc = 1\ ft$$

All other parameters are assumed similar to those in scenario 1.

Second case study (rapid demand change)

This example considers transients caused by rapid demand changes in one of the nodes (solved by Larock *et al.* 1999). This network is supplied by gravity flow from two elevated reservoirs. The pipe and node numbers are shown in Figure 4 with the pipe diameters and lengths. The pressure wave velocity in all pipes is $a = 2{,}800$ ft/sec, and $\Delta x\ and\ \Delta t$ are assumed to be 300 ft and 0.1 sec, respectively.

Scenario 1

In this case, the system is not equipped with a shock damper. Nodes 1 through 4 have ground elevations of 860 ft, while nodes 5 and 6 have ground elevations of 980 ft and 960 ft, respectively. The equivalent sand roughness of all pipes is $e = 0.002$ in. The demand increases from 450 to 900 gal/min at node 2 to meet the sudden need for more water for fire suppression. This effect indicates an increase in demand on the head of node 4.

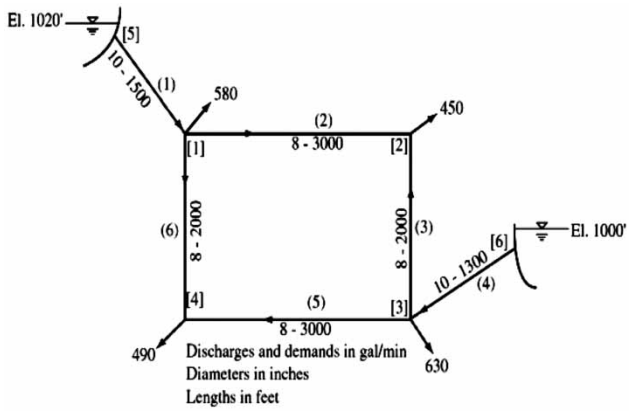

Figure 4 | Schematic of gravity network and parameters in case study 2.

Scenario 2

A shock damper is used in this scenario located 50 ft upstream of node 4. The parameters related to the shock damper are similar to those in the first case study, except the tank diameter here is $Dr = 5$ ft.

RESULTS AND DISCUSSION

As seen in Figures 5 and 6, a water hammer caused by sudden valve closure can generate piezometric heads (and corresponding pressure) of up to 1,200 ft and 100 ft when no shock damper is used. This is relatively severe pressure resulting in extensive damage to the system. Maximum pressure (positive values) can cause pipes to explode. Moreover, the next head peaks reach 1,100 ft and 150 ft due to friction in the pipeline and energy depreciation, although the resulting pressure is high. In this scenario, the impact of the water hammer is still visible after around 300 sec. When a shock damper is utilized as described in scenario 2, the maximum and minimum pressure heads calculated are 720 ft and 540 ft, respectively. This is a greater reduction (40% for the maximum and 80% for the minimum head) compared to scenario 1. Moreover, the peak heads significantly depreciate after almost 50 sec, reaching 650 ft and 550 ft. In the second case study and as indicated in Figure 7, the maximum and minimum pressure heads adjust from 260 ft and 0 ft, respectively, to 165 ft and 55 ft. After about 15 sec, the pressure oscillation also disappears due to the shock damper.

A sensitivity analysis of the system is described herein. The results indicate that shock damper performance is more sensitive to three parameters: main damping coefficient, tank diameter, and shock damper spring stiffness. Tables 1–3 summarize the sensitivity analysis outcome.

Table 1 shows the maximum pressure head obtained at the valve location for damping coefficients of +66% and −66% of its initial value. Evidently, an increase in the damping coefficient decreased the shock damper efficiency, hence a greater piezometric head was generated. Decreasing this

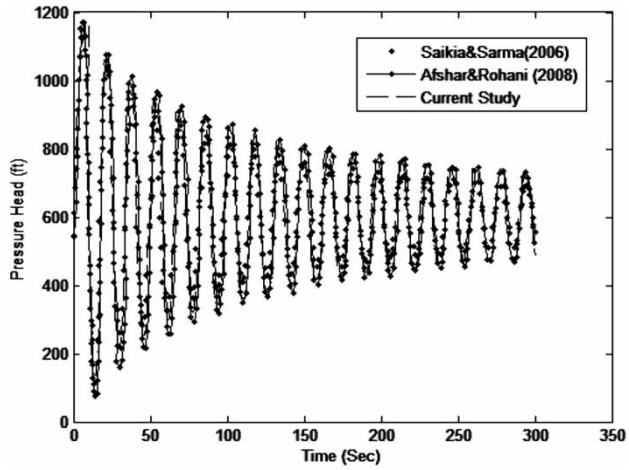

Figure 5 | Pressure head vs time at valve node calculated by previous researchers and in the current work for result fitting (first case study – scenario 1).

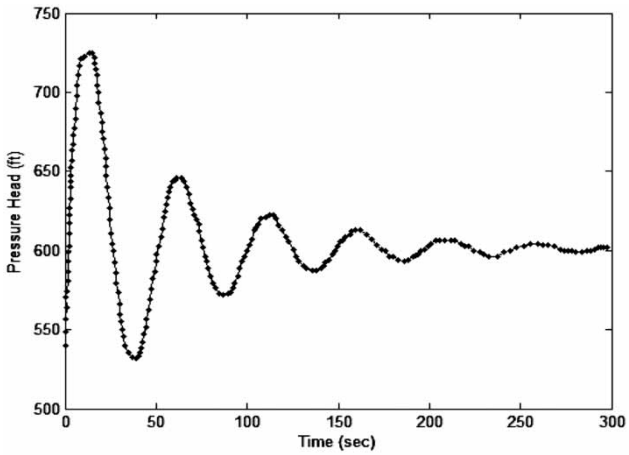

Figure 6 | Pressure head vs time with shock damper at valve node (first case study – scenario 2).

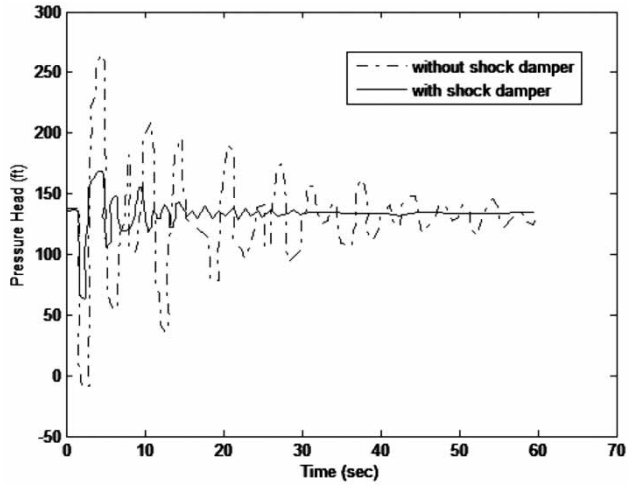

Figure 7 | Pressure head vs time with and without shock damper at node 4 (second case study – scenarios 1 and 2).

Table 1 | Maximum pressure change with damping coefficient ($Dr = 10$ ft and $K_s = 1.4 \times 10^7$ lb/ft)

C (lb.s/ft)	0.5×10^5	1.0×10^5	1.5×10^5	2.0×10^5	2.5×10^5
P_{MAX} (ft)	1,100	988	720	814	1,152

Table 2 | Maximum pressure change with tank diameter ($C = 1.5 \times 10^8$ lb.sec/ft and $K_s = 1.4 \times 10^7$ lb/sec)

Dr (ft)	6	8	10	12	14
P_{MAX} (ft)	1,011	860	720	690	573

Table 3 | Maximum pressure change with spring stiffness ($Dr = 10$ ft and $C = 1.5 \times 10^8$ lb·sec/ft)

K_s (lb/ft)	0.6×10^7	1.0×10^7	1.4×10^7	1.8×10^7	2.8×10^7
P_{MAX} (ft)	1,150	1,023	720	812	990

parameter improved the shock damper's performance. However, a limitation is that further parameter reduction would deteriorate efficiency, suggesting the necessity to seek an optimal level. The system responses to main tank diameter changes are demonstrated in Table 2. As expected, the shock damper performed better with increasing tank size. However, there was a feasible upper limit to this expansion due to physical and economic constraints. Besides, beyond a certain level, any further increase in size appeared to have no considerable effect. Again, this implies there was an optimal level for this capacity expansion. In a situation where the diameter approaches zero, a system with a shock damper and main tank diameter of zero is expected to perform similarly to a system without a shock damper. Table 3 presents the maximum pressure head changes with spring stiffness. The table indicates that an increase and decrease from the optimum values increased the maximum head, so there were optimum values at which the maximum heads could be minimum.

CONCLUSION

Water hammers in water distribution systems are inevitable. Due to the extensive damage caused by this phenomenon, its impact on a system must be moderated efficiently. A shock damper is a simple and economically efficient piece of equipment that can be used to handle devastating consequences such as pipe explosions. The present study concentrated on deriving the governing equation of a shock damper and using it to model the system. Results demonstrated that installing a shock damper in a gravity-feed system can effectively dampen the pressure waves caused by a water hammer. A sensitivity analysis revealed that shock damper performance is mostly dependent on the main tank diameter and the shock damper's damping coefficient. This study also suggests obtaining optimal parameter values in order to maximize performance.

REFERENCES

Afshar, M. H. & Rohani, M. 2008 Water hammer simulation by implicit method of characteristic. *International Journal of Pressure Vessels and Piping* **85** (12), 851–859.

Bergant, A. & Simpson, A. R. 1995 *Water Hammer and Column Separation Measurements in an Experimental Apparatus*. Report No. R128, Dept. of Civil and Environmental Engineering University of Adelaide, Adelaide, Australia.

Chamani, M., Pourshahabi, S. & Sheikholeslam, F. 2013 Fuzzy genetic algorithm approach for optimization of surge tanks. *Scientia Iranica* **20** (2), 278–285.

Chaudhry, H. M. 1979 *Applied Hydraulic Transients*. Springer, New York, USA.

Fathi-Moghadam, M., Haghighipour, S. & Vali Samani, H. M. 2013 Design-variable optimization of hydropower tunnels and surge tanks using a genetic algorithm. *Journal of Water Resources Planning and Management* **139** (2), 200–208.

Ghidaoui, M. S., Zhao, M., McInnis, D. A. & Axworthy, D. H. 2005 A review of water hammer theory and practice. *Applied Mechanics Reviews* **58** (1), 49–76.

Kim, S. H. 2008 Impulse response method for pipeline systems equipped with water hammer protection devices. *Journal of Hydraulic Engineering* **134** (7), 961–969.

Kim, S. H. 2010 Design of surge tank for water supply systems using the impulse response method with the GA algorithm. *Journal of Mechanical Science and Technology* **24** (2), 629–636.

Larock, B. E., Jeppson, R. W. & Watters, G. Z. 1999 *Hydraulics of Pipeline Systems*. CRC Press, New York, USA.

Niełacny, M. 2004 Model of the water-hammer effect considering a spring safety valve. *Archives of Hydro-Engineering and Environmental Mechanics* **51** (1), 25–40.

Saikia, M. D. & Sarma, A. K. 2006 Numerical modeling of water hammer with variable friction factor. *APRN Journal of Engineering and Applied Sciences* **1** (4), 35–40.

Skulovich, O., Bent, R., Judi, D., Perelman, L. S. & Ostfeld, A. 2015 Piece-wise mixed integer programming for optimal sizing of surge control devices in water distribution systems. *Water Resources Research* **51** (6), 4391–4408.

Skulovich, O., Perelman, L. S. & Ostfeld, A. 2016 Optimal closure of system actuators for transient control: an analytical approach. *Journal of Hydroinformatics* **18** (3), 393–408.

Tijsseling, A. 1996 Fluid-structure interaction in liquid-filled pipe systems: a review. *Journal of Fluids and Structures* **10** (2), 109–146.

Tijsseling, A., Vardy, A. & Fan, D. 1996 Fluid-structure interaction and cavitation in a single-elbow pipe system. *Journal of Fluids and Structures* **10** (4), 395–420.

Wylie, E. B. 1984 Fundamental equations of waterhammer. *Journal of Hydraulic Engineering* **110** (4), 539–542.

First received 24 October 2016; accepted in revised form 4 September 2017. Available online 30 October 2017